ACCOUNTS
of chemical research

HOCO Radical Chemistry

JOSEPH S. FRANCISCO*
Department of Chemistry, Purdue University, West Lafayette, Indiana 47907, United States

JAMES T. MUCKERMAN AND HUA-GEN YU*
Department of Chemistry, Brookhaven National Laboratory, Upton, New York 11973, United States

RECEIVED ON JUNE 15, 2010

CONSPECTUS

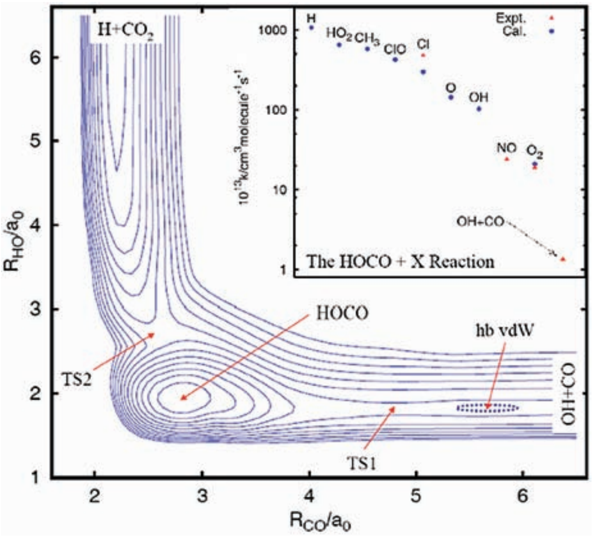

Free radicals are important species in atmospheric chemistry, combustion, plasma environments, interstellar clouds, and biochemistry. Therefore, researchers would like to understand the formation mechanism, structure, stability, reactivity, spectroscopy, and dynamics of these chemical species. However, due to the presence of one or more unpaired electrons, radicals are often very reactive and have short lifetimes, which makes it difficult to conduct experiments. The HOCO radical appears in the atmosphere as well as in combustion environments and plays an important role in the conversion of CO to CO$_2$. Through the interplay between theoretical and experimental investigations, researchers have only recently understood the chemical role of the HOCO radical.

In this Account, we systematically describe the current state of knowledge of the HOCO radical based on recent theoretical and experimental studies. This radical's two stable conformers, *trans*- and *cis*-HOCO, have been identified by high-level ab initio calculations and experimental spectroscopy. *trans*-HOCO is more stable by approximately 1.8 kcal/mol. The heat of formation of HOCO (298 K) was determined to be -43.0 ± 0.5 kcal/mol, giving a potential well depth of 30.1 ± 0.5 kcal/mol relative to the asymptote of the reactants OH + CO. The HOCO radical is very reactive. In most reactions between the HOCO radical and atoms, the HOCO radical acts as a hydrogen donor to reaction partners. Generally, the hydrogen is transferred through the formation of an association intermediate, which then proceeds through a molecular elimination step to produce the reaction products. The reaction rates of HOCO with some small radicals fall in the range of $10^{-11}-10^{-10}$ cm^3 molecule^{-1} s^{-1}. These results clearly illustrate important features in the reactivity of the HOCO radical with other molecules.

I. Introduction

In the atmosphere, the reaction most responsible for the conversion of CO to CO$_2$ is that of OH + CO. This reaction also plays an important role in combustion environments. Over the years, no other reaction has been observed to be as efficient in the conversion of CO to CO$_2$ as the OH + CO → H + CO$_2$ reaction. Prior to the early 1970s, this reaction was believed to be a simple bimolecular reaction. However, an inverse pressure dependence of the OH + CO reaction was observed by Smith and Zellner,[1] who then proposed that the reaction proceeded through the formation of an energized HOCO* radical which could either decompose into reactants, proceed to products, or become thermally stabilized through the collision with a third species. The general reaction mecha-

Published on the Web 10/07/2010 www.pubs.acs.org/acr
10.1021/ar100087v

nism can be expressed as OH + CO ↔ $HOCO^*$ → H + CO_2 and $HOCO^*$ + M → HOCO + M.

This complex mechanism predicts a rate constant behavior that is consistent with the experimentally observed pressure effect[1−3] for a diverse set of buffer gases over a wide range of pressures (0.001−700 bar). The mechanism is also indirectly supported by the deuterium isotope effects on the reaction.[2,4] The strong isotope effect (k_H/k_D) in these studies is found to depend on both the pressure and the third body. For example, at room temperature and in the presence of He gas, the isotope effect is 2.8 at the low pressure limit and 1.6 at high pressures.[2] Based on the mechanism, and the complicated pressure and temperature dependences, the OH + CO reaction has been extensively modeled using variants of the RRKM approach.[3,5−8] These studies show that the reaction is best characterized as a complex-forming bimolecular reaction, and the competitive dissociation of HOCO into either OH + CO or H + CO_2 is responsible for the experimental observations.[9] Real-time clocking experiments using femtosecond laser pump−probe techniques produced the first direct experimental insight into the formation and decay of the HOCO radical from the perspective of the reverse, H + CO_2 → OH + CO, reaction.[10] A number of reviews[8,9] have been published in this area, all of which focus on understanding the details of the OH + CO bimolecular reaction over a variety of experimental conditions. One reason for the paucity of mechanistic work in the area is the obvious complexity of the OH + CO reaction.

This brief history of the OH + CO reaction provides a context for studies in the literature on the HOCO radical. Until recently, the only reactivity studies involving the HOCO radical focused on its reaction with O_2 and NO. New studies of the HOCO reactivity have uncovered the potential for its involvement in other important atmospheric and combustion reactions. To appreciate the significance of HOCO involvement in these reactions, one first has to address several questions such as the existence, structure, lifetime, and reactivity of HOCO. It is only through recent major advances in quantum chemistry and reaction dynamics methods, both experimental and theoretical, that the understanding of these fundamental properties of HOCO has become possible. This Account will focus on important fundamental spectroscopic and dynamical information critical to assessing thermochemical properties, spectroscopy, reaction dynamics, kinetics, and photochemistry, via unimolecular dissociations or bimolecular reactions, into HOCO radical chemistry. Our aim in this Account is to characterize the progress in the field and to highlight the interplay of theory and experiment that have led to improvements in our understanding of HOCO radical chemistry.

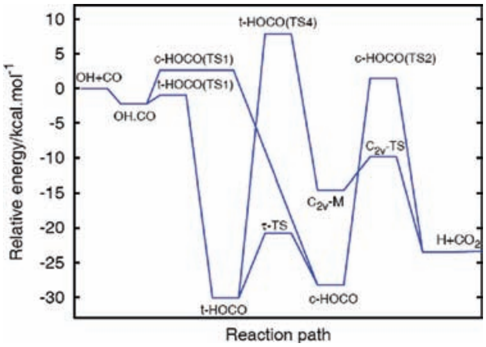

FIGURE 1. Relative electronic energy diagram for the ground-state HOCO radical calculated with the FCC/CBS theory.[15]

TABLE 1. Heat of Formation of HOCO at 298 K

ΔH_f (kcal/mol)	method	ref
-39 ± 7	appearance potential	18
-58 ± 4	appearance potential	19
-53	group additivity	20
-49.8	ab initio	21
-52.5	photoionization	22
$\geq -46.5 \pm 0.7$	photoionization	23
-42.9 ± 1.5	ab initio	12
-42.8	ab initio	15
-43 ± 0.5	ab initio	13

II. Fundamental Properties of HOCO

The HOCO radical has two chemically bound conformers, *trans*-HOCO and *cis*-HOCO, and the metastable isomer HCO_2 (with H−CO_2 connectivity having C_{2V} symmetry). Figure 1 shows critical features on the potential energy surface of HOCO (X^2A'). The equilibrium structures of the minima are well predicted using varieties of ab initio calculations.[11−15] Both conformers have a terminal C═O double bond (1.18−1.19 Å), a central C−O single bond (1.34−1.35 Å), and a typical O−H bond of 0.97 Å with the bond angles of 107° (HOC) and 127°−130° (OCO). The theoretical rotational constants of *trans*-HOCO are consistent with the experimental results from high resolution infrared spectroscopy techniques.[16,17] The far-infrared laser magnetic resonance experiment[17] also confirms that the HOCO radical is stable, with a gas-phase lifetime of 10 ms.

Stability of HOCO. The stability of HOCO has been the subject of a long-standing debate as shown in Table 1. The heat of formation of HOCO was suggested in early work to be about −50 kcal/mol.[18−22] Since Francisco[14] reported a theoretical adiabatic ionization potential of 8.01 eV for HOCO in 1997, the experimental value has been significantly lowered. Ruscic and Litorja[23] reexamined the photoionization spectroscopy of HOCO and revised the adiabatic energy for *trans*-HOCO to be 8.06 ± 0.03 eV from 8.486 ± 0.012 eV.[22] The heat of formation for HOCO is then corrected to be ≥ −46.5 ± 0.7 kcal/mol at room temperature. This new limit is close

TABLE 2. Experimental Frequencies of *trans*-HOCO and *cis*-HOCO

	trans-HOCO			*cis*-HOCO		
mode	cm^{-1}	method	ref	cm^{-1}	method	ref
ν_1(OH str)	3635.702	DFL, gas	30	3316	IR, CO	26
	3628.0	IR, Ne	28			
ν_2(C=O str)	1852.567	DL, gas	29	1797	IR, CO	26
	1848.0	IR, Ne	28			
ν_3(HOC bend)	1211.2	IR, Ar	27	1261	IR, CO	26
ν_4(C−O str)	1050.4	IR, Ne	28	1088	IR, CO	26
ν_5(OCO bend)	615	IR, CO	26	620	IR, CO	26
ν_6(torsion)	508.1	IR, Ne	28			

to the high-level ab initio calculations (about −43.0 kcal/mol)[12,13,15] that correspondingly determine a potential well depth of 30.1 kcal/mol for *trans*-HOCO relative to OH + CO (Figure 1). The adiabatic electron affinity of HOCO[24,25] is obtained as 1.30 eV for *trans*-HOCO and 1.43 eV for *cis*-HOCO. Compared to the electron affinity of the H atom (0.754 eV), both $HOCO^-$ anion conformations are very stable with respect to $H^- + CO_2$ as well as to $OH^- + CO$.

Spectroscopic Properties of HOCO. The fundamental vibrational frequencies of both *trans*- and *cis*-HOCO, as well as their deuterated forms, have been measured by several groups.[26−30] Results are listed in Table 2. Jacox and co-workers[26−28] carried out infrared (IR) absorption spectrum studies in a solid matrix (CO/Ne/Ar) using either UV photolysis or discharge means. The assignment was carefully verified using isotopic substitution studies using both deuterium and ^{18}O. Sears et al.[29] reported a high-resolution laser absorption spectroscopy study of the C=O stretching mode of *trans*-HOCO. Its band origin is precisely measured at $\nu_2 = 1852.567$ cm^{-1} which supports the IR result of 1848.0 cm^{-1} from the low-temperature Ne matrix.[28] They also observed that the rotational levels in this vibrationally excited mode have an irregular dependence on the K_a quantum number, caused by anharmonic interactions with combinations of lower frequency in-plane vibrations. The IR ρ-vibration spectrum of the ν_1 OH stretching mode of *trans*-HOCO has been recorded and assigned by Petty and Moore[30] using IR difference-frequency laser spectroscopy and the photolysis of acrylic acid at 193 nm. The band center, observed at $\nu_1 = 3635.702$ cm^{-1}, is very close to the IR matrix study.[28] In addition, the scaled theoretical harmonic frequencies[11,13−15,25] are also in good agreement with those experiments.

Due to the metastable nature of the HCO_2 isomer, only the OCO bend mode ($\nu_3 = 570$ cm^{-1}) has been measured via the stable HCO_2^- anion using negative-ion photoelectron spectroscopy.[31] Kim et al.[31] found that the first electronically excited state of HCO_2 is nearly degenerate with the ground state.

Two weakly bound linear complexes, HO−CO and HO−OC, were predicted by ab initio calculations.[15,32,33] The existence of the linear OH−CO complex was concretely established by Lester et al.[34] using IR action spectroscopy. The experiments identified the HO−CO complex for the first time by noticing a red shift (29.6 cm^{-1})[34] of the OH overtone in the complex with respect to that in free OH, and by examining the intermolecular energy level pattern owing to the Renner−Teller interaction and spin−orbit coupling. The HO−CO binding energy,[35] $D_0 \le 410$ cm^{-1}, was determined from the quantum state distribution of the OH fragments following vibrational predissociation of HO−CO. Ab initio calculations estimate the OH−CO binding energy to be 405 cm^{-1} (CCSD(T)/aug-cc-pVTZ)[34] and 341 cm^{-1} (FCC/CBS)[15,36] in good accord with the experimental result. The experimental distance (3.936 Å)[35] between the centers of HO and CO is also consistent with the CCSD(T) calculations.[15,34,36] On the other hand, the HO−OC complex is less stable. Its theoretical binding energy was obtained as 240[34] or 101 cm^{-1}.[15] Besides the OH bound complexes, the $H-CO_2$ van der Waals (vdW) complexes were also investigated theoretically.[15,37] Lukes et al.[37] predicted two vdW minima. The more stable one has a perpendicular structure with a well depth of $D_e = 75$ cm^{-1}, while the other is collinear with a well depth of $D_e = 38.0$ cm^{-1}.

The electronic spectrum of HOCO was explored by Milligan and Jacox[26] using 200−300 nm photon energy in a CO matrix at 14 K. No discrete electronic band system was identified for HOCO. Recently, Li and Francisco[11] carried out high-level ab initio studies of the three excited states of HOCO. Vertical excitation energies and potential energy surfaces along the O−H and C−O coordinates show that the first excited state of HOCO is repulsive. In other words, the electronic band of the first excited state may have no discrete structure.

Potential Energy Surfaces of HOCO. The essential molecular feature that connects structural and spectroscopic properties of a chemical entity to its reactivity is the potential energy surface (PES). Knowing the HOCO PES is imperative to understanding the kinetics and dynamics of HOCO reactions. The first global analytic PES for HOCO was constructed by Schatz, Fitzcharles, and Harding[38] (denoted as SFH) in 1987, based on the many-body expansion method of Murrell. A number of researchers have further improved the quality of this surface, mainly by removing some deficiencies of the analytical function and including improved ab initio calculations of stationary points.[15,32] These updated versions of the PES are those of Kudla, Schatz, and Wagner (KSW),[32] Bradley and Schatz (BS),[39] and modifications of the BS surface by

Yu, Muckerman, and Sears (YMS),[15] and Lakin, Troya, Schatz, and Harding (LTSH).[40] By removing the reactant channel well on the LTSH surface, Medvedev et al.[41] produced a mod-LTSH surface. In addition, there is one full-dimensional interpolated surface (Leiden)[42] based on the Shepard interpolation scheme. However, these analytic PESs still require future improvements to suitably reproduce highly accurate ab initio calculations.

III. Reactivity of HOCO

Unimolecular Dissociation of HOCO. The OH + CO reaction has also been studied via the unimolecular dissociation of HOCO radicals. Lester and Pond[35] used IR action spectroscopy to explore the half-reaction OH + CO → HOCO in terms of the hydrogen bound complex HO−CO and its isotopomer DO−CO. They measured the time-resolved decay dynamics of the vibrationally activated HO−CO (or DO−CO) reactant complex with the OH/OD($\nu_{OH} = 2$) fragment. The time scale for overall decay (inelastic scattering and/or chemical reaction) of those complexes was determined to be within 0.19−6 ns. They found two decay pathways to yield inelastically scattered OH ($\nu_{OH} = 1$) products with relatively low/high OH rotational energy, that correlate with CO in $\nu_{CO} = 1/0$ respectively. These decay pathways are firmly supported by Gray et al.[43] carrying out a full dimensional quantum dynamics calculation based on both the *A′* and *A″* PESs of LTSH.[40] In addition, Yu and Muckerman[44] performed a photodissociation dynamics study of the OH overtone ($\nu_{OH} = 3$) of *trans*-HOCO using a time-dependent wave packet approach. The lifetime of the vibrationally excited HOCO radicals was estimated to be 0.94−3.1 ps. The energized radicals can dissociate into both OH + CO and H + CO_2 products, where the latter is the minor channel with a branching fraction of 0.12−0.33.

Continetti and co-workers[24,25,45] reported a series of coincidence studies of the photoelectron-photofragment angular distributions in the one- and two-photon dissociative photodetachment (DPD) of $HOCO^-$, $HOCO^- + h\nu \rightarrow HOCO + e^-$, at photon energies of 386 and 258 nm. Since the spectrum of the translational energy partitioning among photoelectron and photofragments is coincidently measured from the same DPD event, those measurements provide deep insight into the dissociation dynamics on the involved PESs. In the DPD dynamics, the nascent HOCO radicals are mostly (more than two-thirds) stabilized,[24] which is consistent with the deep well feature on the PES. The radical lifetime[45] was examined as a function of the orientation of the transition dipole, with upper limits of 0.9 ps for the HOCO lifetime (or 1.3 ps for DOCO) for dissociation into OH (OD) + CO. Importantly, isotopic substitution by deuterium in the parent anion is observed to reduce the product branching ratio for the D + CO_2 channel, consistent with the role tunneling plays in this dissociation pathway.

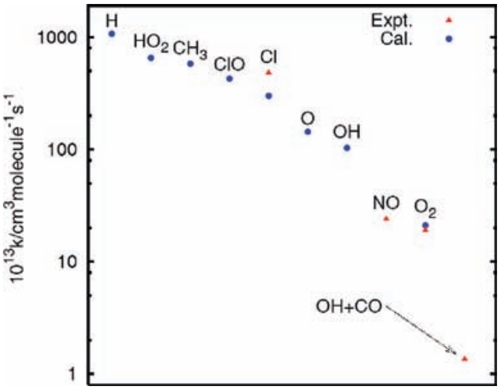

FIGURE 2. Experimental (red triangles) and theoretical (blue circles) rate coefficients for HOCO + *X* (labeled in the figure) reactions at room temperature for various species *X*. Also shown for comparison is the rate constant for the OH + CO → H + CO_2 reaction.

The DPD dynamics of $HOCO^-$ at 258 nm were simulated by Gray et al.[46] using a six-dimensional wave packet approach on the LTSH surface of HOCO.[40] A variety of observables were determined: the electron kinetic energy (eKE) distributions associated with the OH + CO and H + CO_2 channels, the correlated eKE and product translational energy distribution for the OH + CO channel, and product branching ratios. Most results are in good accord with the experimental results of Clements et al.[25] except that the calculated eKE distribution for the H + CO_2 channel is noticeably colder than the experimental value. One (partial) reason for this discrepancy may be an inadequate description of the barrier region of the PES to form H + CO_2, where the LTSH barrier is too thick, resulting in the suppression of tunneling in the LTSH surface.

Bimolecular Reactions of HOCO. There exist only a handful of theoretical and experimental investigations on the reaction of HOCO with other molecules and atoms. A summary is presented in Figure 2 of the thermal rate coefficients at room temperature for the systems that have been studied. These radical−radical reactions are very fast. In general, their thermal rate coefficients are 2−3 orders of magnitude lager than that of the OH + CO reaction; exceptions are the reactions of HOCO with O_2 and NO, for which there is a small classical barrier in the entrance channels. Even so, their rate coefficients are still about 20 times larger.

As HOCO is an active free radical, in experimental studies, one needs to prepare HOCO in the reaction environment. In general, there are two major approaches: the ultraviolet photodissocation[47] of acrylic acid or trifluoroacetic acid, and the reaction of formic acid with chlorine[3,49,50] or fluorine[22] atoms. The HOCO radicals produced by the reactive sources have small excess energy (e.g., 13.0 kcal/mol for Cl + HCOOH), and were found to be stable with a very long lifetime (≥10 ms) at room temperature.[49] Both techniques have been used to study the reaction of HOCO with O_2, NO and Cl.

The O_2 + HOCO reaction has been well studied, both experimentally and theoretically. Experimental measurements were first carried out by Moore et al.[47] and Nolte et al.[50] in 1993 and then by Miyoshi et al.[49] At room temperature and pressures up to approximately 2.0 mbar, Notle et al.[50] determined a thermal rate coefficient of 1.64 (±0.25) × 10^{-12} cm^3 $molecule^{-1}$ s^{-1} using far IR laser magnetic resonance detection of HOCO. Miyoshi et al.[49] predicted a slightly smaller thermal rate coefficient of 1.44 (±0.3) × 10^{-12} cm^3 $molecule^{-1}$ s^{-1} using a photoionoization mass spectroscopy method to detect HOCO. In both experiments, the HOCO reactants were produced by the Cl + HCOOH reaction in a flow system. Moore et al.,[47] on the other hand, employed a spectroscopic method to investigate the kinetics of O_2 + HOCO in which the *trans*-HOCO radicals were produced by 193 nm photolysis of acrylic acid. At $T = 293$ K and low pressures (2.3−9.8 Torr), they obtained a thermal rate coefficient of 1.9 (±0.2) × 10^{-12} cm^3 $molecule^{-1}$ s^{-1}. For the isotopic reaction O_2 + DOCO, the corresponding value was predicted to be 1.8 (±0.2) × 10^{-12} cm^3 $molecule^{-1}$ s^{-1}. This suggests that the reaction lacks an H/D isotope dependence, leading them to deduce that the O_2 + HOCO reaction occurs via an intermediate complex. In addition, it is also found that the reactions of HOCO with CO, C_2H_4, and C_2H_2 are rather slow, with a thermal rate coefficient less than 3 × 10^{-14} cm^3 $molecule^{-1}$ s^{-1}.

The detailed reaction pathways for the O_2 + HOCO reaction have been characterized by Poggi and Francisco[51] using the QCISD(T) method. Consistent with the predictions of Moore et al.,[47] it was determined that the only products are HO_2 + CO_2 which can be produced through two reaction pathways with a small barrier. The first is the direct hydrogen abstraction reaction (with a barrier height of 3.5 kcal/mol); the other is through an addition reaction mechanism (with a barrier of 1.6 kcal/mol) via the $HOC(O)O_2$ intermediate. Due to the small dissociation barrier (4.8 kcal/mol) of $HOC(O)O_2$, the lifetime of the intermediate is very short, about 0.66 ps determined from the direct ab initio molecular dynamics calculations.[52] In the dynamics study, both reaction mechanisms were confirmed although the addition mechanism was found to be preferred. The dynamics calculations gave a room-temperature thermal rate coefficient of 2.1 × 10^{-12} cm^3 $molecule^{-1}$ s^{-1} with a small positive activation energy of 0.7 kcal/mol.

The kinetics of the NO + HOCO reaction have been investigated by Moore et al.[47] and Smith et al.[53] The experimental results[47] showed that this reaction resembles the O_2 + HOCO reaction, having a thermal rate coefficient of 2.45 × 10^{-12} cm^3 $molecule^{-1}$ s^{-1} at 293 K and lacking an H/D isotopic dependence. According to the reaction energetics, Moore et al. suggest two potential product channels: (a) HONO + CO and (b) HNO + CO_2. However, the ab initio calculations[51] exclude the first of these due to the high exit barrier. In contrast, the rate-limited step in the addition reaction mechanism is determined by the dissociation of the HOC(O)NO intermediate into HNO + CO_2 instead of an entrance barrier. The unimolecular dissociation barrier is slightly higher than the asymptote of the reactants. Therefore, HOC(O)NO should be a long-lived intermediate. Similarly, the same feature was also noticed for the NO_2 + HOCO reaction.[54]

Another experimentally studied example is the Cl + HOCO reaction.[48] Experimental results showed that the reaction is quite fast and produces only the HCl + CO_2 products. At room temperature, the rate coefficient is determined to be 4.8 (±1.0) × 10^{-11} cm^3 $molecule^{-1}$ s^{-1}. The experimental observations have recently been confirmed by the molecular dynamics calculations.[55] The calculated rate coefficient is 3.0 × 10^{-11} cm^3 $molecule^{-1}$ s^{-1} (298 K) with a negative activation energy of −0.2 kcal/mol in the temperature range of 200−600 K. Surprisingly, trajectories demonstrate that the Cl + HOCO → HCl + CO_2 reaction occurs via a dual-path complex-formation mechanism characterized by very short-lived (0.31 ps) and moderately long-lived (1.9 ps) complexes, both involving the addition of Cl to HOCO. No direct hydrogen abstraction trajectory was found. This unusual mechanism was suggested to be the result of poor vibration−vibration energy transfer in the newly formed HOC(O)Cl complex.

There have been several theoretical dynamics and/or kinetics investigations on the reactions of the HOCO radical with other small radicals, such as H, O, OH, ClO, HO_2, and CH_3 radicals.[56−61] The principal results from these studies are given in Table 3. In general, the HOCO radical acts as a hydrogen donor to the reaction partner; the reactions release a large amount of energy; the addition reaction mechanism via an intermediate complex prevails; and the temperature dependence of the thermal rate coefficients is rather weak.

The O + HOCO reaction[56] occurs via the direct H abstraction and/or addition reaction mechanisms but has a larger rate coefficient (1.44 × 10^{-11} cm^3 $molecule^{-1}$ s^{-1} at $T = 298$ K). The HOC(O)O intermediate is very short-lived, and only the OH + CO_2 products are yielded. Among all the tabulated reactions, the H + HOCO reaction is the fastest, and this is par-

TABLE 3. Complex Stability, Major Products, and Their Product Branching Fractions for the X + HOCO Reactions

	complex		products			
reactants	D_0[a]	lifetime (ps)	fragments	reaction enthalpy (0 K)	fraction	ref
Cl + HOCO	97.8	1.9	HCl + CO_2	−100.7	1.0	48, 55
H + HOCO	96.6		H_2O+ CO	−101.7	0.99	57
			H_2 + CO_2	−91.2	0.01	
O + HOCO	94.5	0.17	OH + CO_2	−98.6	1.0	56
			HO_2 + CO	−39.7	0.0	
O_2 + HOCO	38.2	0.66	HO_2 + CO_2	−46.8	1.0	47, 49−52
NO + HOCO	32.8		HNO + CO_2	−45.9	1.0	47, 51, 53
			HONO + CO	−22.2	0.0	
OH + HOCO	108.1		H_2O + CO_2	−116.0	1.0	58
ClO + HOCO	84.3	<4.0	HOCl + CO_2	−91.6	0.467	60
			HCl + CO_3	−41.8	0.01	
			Cl + HOC(O)O	−41.2	0.52	
			HClO + CO_2	−39.8	0.003	
HO_2 + HOCO	78.5	0.88	H_2O_2 + CO_2	−84.6	0.77	59
			H_2O + CO_3	−55.1	0.056	
			HCOOH + $^3O_2$	−48.3	0.01	
			OH + HOC(O)O	−38.5	0.15	
			HCOOH + $^1O_2$	−25.7	0.019	
CH_3 + HOCO	91.8	4500	CH_4 + CO_2	−101.9	0.39	61
			CH_2CO + H_2O	−59.8	0.61	

[a] The binding energy in kcal/mol is relative to the reactants.

tially due to the light reduced mass. This reaction can produce two sets of products: H_2O + CO and H_2 + CO_2. The rate coefficients and product branching ratios were reported in the temperature range of 200−1000 K.[57] At room temperature, the rate coefficient is predicted to be 1.07×10^{-10} cm^3 molecule^{-1} s^{-1}, with branching fractions of 0.99 for (H_2O + CO) and 0.01 for (H_2 + CO_2). The thermal rate coefficients are nearly temperature independent. However, the product branching ratios have noticeable temperature dependence with the slight preference of H_2 + CO_2 products at high temperatures.

Dynamics calculations[58] show that hydrogen bonding may play an important role in the OH + HOCO reaction, especially at low temperatures. At room temperature, the calculated thermal rate coefficient is 1.0×10^{-11} cm^3 molecule^{-1} s^{-1}, or nearly 2 orders of magnitude larger than that for the OH + CO reaction. Therefore, the OH + HOCO reaction has important ramifications for the removal of HOCO radicals in both atmospheric and combustion processes, and has apparent implications for the lifetime of the HOCO radical in laboratory studies. In other words, the two-step reaction mechanism, (a) OH + CO → HOCO and (b) OH + HOCO → H_2O + CO_2, becomes competitive with the one-step OH + CO → H + CO_2 reaction for the oxidation of CO to CO_2 involving OH radicals.

Yu and Francisco[61] carried out a combined direct ab initio molecular dynamics/RRKM study on the CH_3 + HOCO reaction at $T \leq 1000$ K. The obtained thermal rate coefficient was 5.8×10^{-11} cm^3 molecule^{-1} s^{-1} at room temperature. In particular, the reaction was predicted to produce more H_2O + CH_2CO (61%) products than the most exothermic products CH_4 + CO_2 (39%). A similar behavior was also noticed for the HO_2 + HOCO reaction[59] as shown in Table 3. Although the H_2O_2 + CO_2 products dominate, the product branching fraction for OH + HOC(O)O is as high as 0.15, exceeding that of both (H_2O + CO_3) and HOC(O)H + $O_2(X^3\Sigma)$. The overall rate coefficient obtained was 6.5×10^{-11} cm^3 molecule^{-1} s^{-1}, at room temperature. Such diversity of products in the HO_2 + HOCO reaction comes from the fact that the reaction is able to occur on the excited triplet potential energy surface.

The ClO + HOCO reaction[60] was investigated using a variational RRKM approach in the temperature range 200−1000 K. At room temperature, the thermal rate coefficient is 4.26×10^{-12} cm^3 molecule^{-1} s^{-1} with negative temperature dependence. The product branching fractions were predicted to be Cl (0.518), HOCl (0.469), HCl (0.01), and HClO (0.003). Interestingly, the fact that the ClO + HOCO reaction produces nearly equally amounts of Cl and HOCl suggests that the ClO + HOCO reaction could be a new radical reaction that performs the same functions as the ClO + HO_x reactions in the depletion of ozone as well as the conversion of CO into CO_2.

IV. Conclusions

This Account summarizes the recent studies of the HOCO radical, an important transient intermediate in the atmosphere and combustion systems. This radical has two stable conformers: *trans*- and *cis*-HOCO, with *trans*-HOCO being more stable by about 1.8 kcal/mol. Both conformers have been identified by high-level ab initio calculations and experimental spectroscopy. The heat of formation of HOCO (298 K) was determined to be −43.0 ± 0.5 kcal/mol, giving a potential well depth of 30.1 ± 0.5 kcal/mol relative to the OH + CO asymptote.

It is also evident that the HOCO radical is very reactive. A general feature of HOCO reactions with atoms and radicals is that the HOCO radical acts as a hydrogen donor to reaction partners. The mechanism by which the hydrogen is transferred is generally through the formation of an association intermediate, which then proceeds through a molecular elimination step to produce the reaction products. The reaction rates of HOCO with some small radicals fall in the range of $10^{-11}-10^{-10}$ cm^3 molecule^{-1} s^{-1}. These results clearly illustrate that the HOCO radical can play an important role in its reactivity with other molecules.

The work done at Brookhaven National Laboratory was supported by the Division of Chemical Sciences, Office of Basic Energy Sciences of the U.S. Department of Energy under Contract No. DE-AC02-98CH10886.

BIOGRAPHICAL INFORMATION

Joseph S. Francisco is the William E. Moore Distinguished Professor of Earth and Atmospheric Science and Chemistry at Purdue University. He received his B.S. degree at the University of Texas at Austin and his Ph.D. degrees from the Massachusetts Institute of Technology, and did his postdoctoral training at Cambridge University. His research interests are primarily in the areas of spectroscopy, chemical kinetics, computational chemistry, and atmospheric chemistry.

James T. Muckerman received his B.S. degree from Carleton College and Ph.D. from the University of Wisconsin. He joined Brookhaven National Laboratory as an Associate Chemist and currently is a Senior Chemist. His research interest focus on theoretical dynamics of reactive collisions and photodissociation processes with emphasis on combined quantum/classical approaches for treating the dynamics of large molecular systems.

Hua-Gen Yu received his B.S. degree from Chengdu University of Sciences and Technology (presently Sichuan University) of China and Ph.D. in 2000 from the Göteborg University, Sweden. He then joined Brookhaven National Laboratory as a Goldhaber distinguished postdoctoral fellow and now is a Chemist. His research interests focus on the theory and computation of the dynamics of chemical reactions and molecular spectroscopy.

FOOTNOTES

*To whom correspondence should be addressed. E-mail: francisc@purdue.edu; hgy@bnl.gov.

REFERENCES

1 Smith, I. W. M.; Zellner, R. Rate Measurements of Reactions of OH by Resonance Absorption. Part 2. Reactions of OH with CO, C_2H_4 and C_2H_2. *J. Chem. Soc., Faraday Trans. II* **1973**, *69*, 1617–1627.

2 Frost, M. J.; Sharkey, P.; Smith, I. W. M. Reaction Between OH (OD) Radicals and CO at Temperatures Down to 80 K - Experiment and Theory. *J. Phys. Chem.* **1993**, *97*, 12254–12259.

3 Fulle, D.; Hamann, H. F.; Hippler, H.; Troe, J. High Pressure Range of Addition Reactions of HO. 2. Temperature and Pressure Dependence of the Reaction HO + CO ↔ HOCO → H + CO_2. *J. Chem. Phys.* **1996**, *105*, 983–1000.

4 Golden, D. M.; Smith, G. P.; McEwen, A. B.; Yu, C.-L.; Eiteneer, B.; Frenklach, M.; Vaghjiani, G. L.; Ravishankara, A. R.; Tully, F. P. OH (OD) + CO: Measurements and an Optimized RRKM Fit. *J. Phys. Chem. A* **1998**, *102*, 8598–8606.

5 Zhu, R. S.; Diau, E. G. W.; Lin, M. C.; Mebel, A. M. A Computational Study of the OH (OD) + CO Reactions: Effects of Pressure, Temperature, and Quantum-Mechanical Tunneling on Product Formation. *J. Phys. Chem. A* **2001**, *105*, 11249–11259.

6 Senosiain, J. P.; Klippenstein, S. J.; Miller, J. A. A Complete Statistical Analysis of the Reaction Between OH and CO. *Proc. Combust. Inst.* **2005**, *30*, 945–953.

7 Joshi, A. V.; Wang, H. Master Equation Modeling of Wide Range Temperature and Pressure Dependence of CO + OH Reactions. *Int. J. Chem. Kinet.* **2006**, *38*, 57–73.

8 Marcus, R. A. Mass-Independent Oxygen Isotope Fractionation in Selected Systems. Mechanistic Considerations. *Adv. Quantum Chem.* **2008**, *55*, 5–19.

9 Barker, J. R.; Golden, D. M. Master Equation Analysis of Pressure-Dependent Atmospheric Reactions. *Chem. Rev.* **2003**, *103*, 4577–4591.

10 Scherer, N. F.; Sipes, C.; Bernstein, R. B.; Zewail, A. H. Real-Time Clocking of Bimolecular Reactions - Application to H + CO_2. *J. Chem. Phys.* **1990**, *92*, 5239–5259.

11 Li, Y. M.; Francisco, J. S. High Level Ab Initio Studies on the Excited States of HOCO Radical. *J. Chem. Phys.* **2000**, *113*, 7963–7970.

12 Duncan, T. V.; Miller, C. E. The HCO_2 Potential Energy Surface: Stationary Point Energetics and the HOCO Heat of Formation. *J. Chem. Phys.* **2000**, *113*, 5138–5140.

13 Feller, D.; Dixon, D. A.; Francisco, J. S. Coupled Cluster Theory Determination of the Heats of Formation of Combustion-Related Compounds: CO, HCO, CO_2, HCO_2, HOCO, HC(O)OH, and HC(O)OOH. *J. Phys. Chem. A* **2003**, *107*, 1604–1617.

14 Francisco, J. S. Molecular Structure, Vibrational Frequencies, and Energetics of the $HOCO^+$ Ion. *J. Chem. Phys.* **1997**, *107*, 9039–9045.

15 Yu, H. G.; Muckerman, J. T.; Sears, T. J. A Theoretical Study of the Potential Energy Surface for the Reaction OH + CO → H + CO_2. *Chem. Phys. Lett.* **2001**, *349*, 547–554.

16 Radford, H. E.; Moore, M. A.; Sears, T. J.; Grussdorf, J.; Nolte, J.; Temps, F. Far-Infrared Laser Magnetic-Resonance of X^2A' Trans-DOCO. *J. Mol. Spectrosc.* **1994**, *165*, 137–149.

17 Sears, T. J.; Radford, H. E.; Moore, M. A. B-Dipole Transitions in Trans-HOCO Observed by Far-Infrared Laser Magnetic-Resonance. *J. Chem. Phys.* **1993**, *98*, 6624–6631.

18 Bernecker, R.; Long, F. A. Heats of Formation of Some Organic Positive Ions and Their Parent Radicals and Molecules. *J. Phys. Chem.* **1961**, *65*, 1565–1569.

19 Haney, M. A.; Franklin, J. L. Excess Energies in Mass Spectra of Some Oxygen-Containing Organic Compounds. *Trans. Faraday Soc.* **1969**, *65*, 1794–1804.

20 O'Neal, H. E.; Benson, S. W. In *Free Radicals*; Kochi, J. K., Ed.; Wiley-Interscience: New York, 1973; Vol. 2.

21 Schatz, G. C. The Analytical Representation of Electronic Potential Energy Surfaces. *Rev. Mod. Phys.* **1989**, *61*, 669–688.

22 Ruscic, B.; Schwarz, M.; Berkowitz, J. A Photo-ionization Study of the COOH Species. *J. Chem. Phys.* **1989**, *91*, 6780–6785.

23 Ruscic, B.; Litorja, M. Photo-ionization of HOCO Revisited: a New Upper Limit to the Adiabatic Ionization Energy and Lower Limit to the Enthalpy of Formation. *Chem. Phys. Lett.* **2000**, *316*, 45–50.

24 Lu, Z.; Hu, Q. C.; Oakman, J. E.; Continetti, R. E. Dynamics on the HOCO Potential Energy Surface Studied by Dissociative Photodetachment of $HOCO^-$ and DOCO. *J. Chem. Phys.* **2007**, *126*, 194305.

25 Clements, T. G.; Continetti, R. E.; Francisco, J. S. Exploring the OH + CO → H + CO_2 Potential Surface via Dissociative Photodetachment of $HOCO^-$. *J. Chem. Phys.* **2002**, *117*, 6478–6488.

26 Milligan, D. E.; Jacox, M. E. Infrared Spectrum and Structure of Intermediates in Reaction of OH with CO. *J. Chem. Phys.* **1971**, *54*, 927–942.

27 Jacox, M. E. The Vibrational-Spectrum of the trans-HOCO Free-Radical Trapped in Solid Argon. *J. Chem. Phys.* **1988**, *88*, 4598–4607.

28 Forney, D.; Jacox, M. E.; Thompson, W. E. Infrared Spectra of trans-HOCO, $HCOOH^+$, and HCO_2^- Trapped in Solid Neon. *J. Chem. Phys.* **2003**, *119*, 10814–10823.

29 Sears, T. J.; Fawzy, W. M.; Johnson, P. M. Transient Diode-Laser Absorption-Spectroscopy of the ν_2 Fundamental of trans-HOCO and DOCO. *J. Chem. Phys.* **1992**, *97*, 3996–4007.

30 Petty, J. T.; Moore, C. B. Transient Infrared-absorption Spectrum of the ν_1 Fundamental of trans-HOCO. *J. Mol. Spectrosc.* **1993**, *161*, 149–156.

31 Kim, E. H.; Bradforth, S. E.; Arnold, D. W.; Metz, R. B.; Neumark, D. M. Study of HCO_2 and DCO_2 by Negative-Ion Photoelectron-Spectroscopy. *J. Chem. Phys.* **1995**, *103*, 7801–7814.

32 Kudla, K.; Koures, A. G.; Harding, L. B.; Schatz, G. C. A Quasi-Classical Trajectory Study of OH Rotational-Excitation in OH+CO Collisions Using Ab Initio Potential Surfaces. *J. Chem. Phys.* **1992**, *96*, 7465–7473.

33 Spelsberg, D. Dynamic Multipole Polarizabilities and Reduced Spectra for OH, Application to the Long-Range Part of the Two Lowest Potential Surfaces of the OH-CO Complex. *J. Chem. Phys.* **1999**, *111*, 9625–9633.

34 Lester, M. I.; Pond, B. V.; Anderson, D. T.; Harding, L. B.; Wagner, A. F. Exploring the OH + CO Reaction Coordinate via Infrared Spectroscopy of the OH-CO Reactant Complex. *J. Chem. Phys.* **2000**, *113*, 9889–9892.

35 Pond, B. V.; Lester, M. I. Decay Dynamics of the Vibrationally Activated OH-CO Reactant Complex. *J. Chem. Phys.* **2003**, *118*, 2223–2234.

36 Botschwina, P. *Faraday Discuss. Chem. Soc.* **2001**, *118*, 424.

37 Lukes, V.; Ilcin, M.; Laurinc, V.; Biskupic, S. On the Structure and Physical Origin of Weak Interaction Between H and CO_2. *Chem. Phys.* **2003**, *290*, 93–100.

38 Schatz, G. C.; Fitzcharles, M. S. State-to-state Chemistry with Fast Hydrogen Atoms Reaction and Collisional Excitation in H + CO. *Faraday Disc. Chem. Soc.* **1987**, *84*, 359.

39 Bradley, K. S.; Schatz, G. C. A Quasiclassical Trajectory Study of H + CO_2: Angular and Translational Distributions, and OH Angular Momentum Alignment. *J. Chem. Phys.* **1997**, *106*, 8464–8472.

40 Lakin, M. J.; Troya, D.; Schatz, G. C.; Harding, L. B. A Quasiclassical Trajectory Study of the Reaction $OH + CO \rightarrow H + CO_2$. *J. Chem. Phys.* **2003**, *119*, 5848–5859.

41 Medvedev, D. M.; Gray, S. K.; Goldfield, E. M.; Lakin, M. J.; Troya, D.; Schatz, G. C. Quantum Wave Packet and Quasiclassical Trajectory Studies of OH+CO: Influence of the Reactant Channel Well on Thermal Rate Constants. *J. Chem. Phys.* **2004**, *120*, 1231–1238.

42 Valero, R.; van Hemert, M. C.; Kroes, G. J. Classical Trajectory Study of the HOCO System Using a New interpolated Ab Initio Potential Energy Surface. *Chem. Phys. Lett.* **2004**, *393*, 236–244.

43 He, Y.; Goldfield, E. M.; Gray, S. K. Quantum Dynamics of Vibrationally Activated OH-CO Reactant Complexes. *J. Chem. Phys.* **2004**, *121*, 823–828.

44 Yu, H. G.; Muckerman, J. T. Quantum Dynamics of the Photoinitiated Unimolecular Dissociation of HOCO. *J. Chem. Phys.* **2002**, *117*, 11139–11145.

45 Lu, Z.; Oakman, J. E.; Hu, Q. C.; Continetti, R. E. Photoelectron-Photofragment Angular Correlations in the Dissociative Photodetachment of HOCO. *Mol. Phys.* **2008**, *106*, 595–606.

46 Zhang, S.; Medvedev, D. M.; Goldfield, E. M.; Gray, S. K. Quantum Dynamics Study of the Dissociative Photodetachment of $HOCO^-$. *J. Chem. Phys.* **2006**, *125*, 164312.

47 Petty, J. T.; Harrison, J. A.; Moore, C. B. Reactions of trans-HOCO Studied by Infrared-Spectroscopy. *J. Phys. Chem.* **1993**, *97*, 11194–11198.

48 Osborne, M. C.; Li, Q.; Smith, I. W. M. Products of the Ultraviolet Photodissociation of Trifluoroacetic Acid and Acrylic Acid. *Phys. Chem. Chem. Phys.* **1999**, *1*, 1447–1454.

49 Miyoshi, A.; Matsui, H.; Washida, N. Detection and Reactions of the HOCO Radical in Gas-Phase. *J. Chem. Phys.* **1994**, *100*, 3532–3539.

50 Nolte, J.; Grussdorf, J.; Temps, E.; Wagner, H. G. Kinetics of the Reaction HOCO + O_2 in the Gas-Phase. *Z. Naturforsch., A: Phys. Sci.* **1993**, *48*, 1234–1238.

51 Poggi, G.; Francisco, J. S. An Ab Initio Study of the Competing Reaction Channels in the Reaction of HOCO Radicals with NO and O_2. *J. Chem. Phys.* **2004**, *120*, 5073–5080.

52 Yu, H. G.; Muckerman, J. T. Quantum Molecular Dynamics Study of the Reaction of O_2 with HOCO. *J. Phys. Chem. A* **2006**, *110*, 5312–5316.

53 Olkhov, R. V.; Li, Q.; Osborne, M. C.; Smith, I. W. M. Branching Ratios for Competing Channels in the Reaction of HOCO Radicals with NO. *Phys. Chem. Chem. Phys.* **2001**, *3*, 4522–4528.

54 Poggi, G.; Francisco, J. S. An Ab Initio Study of the Reaction of HOCO Radicals with NO_2: Addition/Elimination Mechanism. *J. Chem. Phys.* **2009**, *130*, 124306.

55 Yu, H. G.; Francisco, J. S.; Muckerman, J. T. Ab Initio and Direct Dynamics Study of the Reaction of Cl Atoms with HOCO. *J. Chem. Phys.* **2008**, *129*, 064301.

56 Yu, H. G.; Muckerman, J. T.; Francisco, J. S. Quantum Force Molecular Dynamics Study of the Reaction of O Atoms with HOCO. *J. Chem. Phys.* **2007**, *127*, 094302.

57 Yu, H. G.; Francisco, J. S. Energetics and Kinetics of the Reaction of HOCO with Hydrogen Atoms. *J. Chem. Phys.* **2008**, *128*, 244315.

58 Yu, H. G.; Muckerman, J. T.; Francisco, J. S. Direct Ab Initio Dynamics Study of the OH Plus HOCO Reaction. *J. Phys. Chem. A* **2005**, *109*, 5230–5236.

59 Yu, H. G.; Poggi, G.; Francisco, J. S.; Muckerman, J. T. Energetics and Molecular Dynamics of the Reaction of HOCO with HO_2 Radicals. *J. Chem. Phys.* **2008**, *129*, 214307.

60 Yu, H. G.; Francisco, J. S. Ab Initio and RRKM Study of the Reaction of ClO with HOCO Radicals. *J. Phys. Chem. A* **2009**, *113*, 12932–12941.

61 Yu, H. G.; Francisco, J. S. Theoretical Study of the Reaction of CH_3 with HOCO Radicals. *J. Phys. Chem. A* **2009**, *113*, 3844–3849.